

Dynamic Analysis of SSI Effects on Underground Structures



Vijay Kumar, Mithilesh Kumar, Madan Kumar, and Akash Priyadarshree

Abstract This paper describes the Dynamic Soil-Structure Interaction (SSI) effects on the underground structures. The finite element model for Nuclear Power Plant (NPP) and a tunnel was considered to analyze the effects of SSI. Dynamic analysis was carried out considering three transmitting boundary conditions. The effect of embedment for NPP founded on soft soil and seismic responses of a reinforced concrete building in proximity with an underground circular tunnel were studied. The lateral spacing of the circular tunnel from the center line of the building was varied while maintaining a constant depth below the ground level. The effect of embedment has been investigated and the result shows acceleration and displacement responses of the system are smaller with the infinite boundary as compared to viscous and kelvin boundary conditions. In tunnel analysis, the results shows maximum building response occurs when the tunnel is positioned directly below the centre line of the building.

Keywords SSI · Transmitting boundaries · Underground structures · Embedment

1 Introduction

The process in which the motion of the soil influences the response of the structure and the motion of the structure influences the response of the soil is termed as soil-structure interaction (SSI). The soil-structure interaction effect plays an important role in the seismic analysis of infrastructure and industrial facilities, especially for underground structures. It is more observed when massive or elevated structures are situated at soft soil thus it is one of the most widely studied phenomena in earthquake engineering. Over the past four decades, broad research has been performed to study

V. Kumar (✉) · A. Priyadarshree
Muzaffarpur Institute of Technology, Muzaffarpur 842003, India

M. Kumar
Saharsa College of Engineering, Saharsa 852201, India

M. Kumar
Government Polytechnic, Muzaffarpur 842001, Bihar, India

the phenomenon of SSI, and its impact on the seismic response of structures. One of the major challenges in the analysis of dynamic soil-structure interaction problems is to achieve stable and economical modeling. In the numerical simulation of wave propagation problems by finite element, it is necessary to eliminate the boundary events which are generated by the boundary of the numerical grids. Artificial boundaries in numerical analysis generally introduce spurious reflected waves. The numerical modeling of waves in underground structures is a challenging task for several reasons. One of the primary obstacles is formulating an accurate yet inexpensive procedure for dynamic interaction analysis is the modeling of unbounded medium beneath the structures. Many approaches of modeling have been developed in both time and frequency domains. A critical review of the existing literature suggests that various available techniques could be grouped into the following two major categories:

- (a) Rigorous Approach,
- (b) Approximate Approach.

A rigorous approach which is global in space and time: first solving in the frequency domain and then in the time domain. To obtain a solution in the time domain, the procedures involve the convolution process, which uses Fourier transform. Therefore, these have no errors other than discretization and truncation errors. In this modeling approach, radiation condition is exactly satisfied at infinity. On the basis of the review of literature, the following rigorous boundaries can be reckoned:

- (i) Consistent Boundary [1],
- (ii) Boundary Element Method [2],
- (iii) Consistent Infinitesimal Finite Element Cell Method [3],
- (iv) Scaled Boundary Finite Element Method [4],
- (v) Perfectly Matched Layer [5].

Approximate approach boundaries are used in the direct method of analysis in the time domain. As we know that most of the transmitting boundaries are simple in their formulation in the time domain and can be easily implemented in finite element code. On the basis of the review of literature, the following approximate boundaries could be cited:

- (i) Viscous Boundary [6],
- (ii) Paraxial Boundary [7],
- (iii) Superposition Boundary [8],
- (iv) Infinite Element [9],
- (v) Extrapolation Algorithm [10],
- (vi) Transient Transmitting Boundary [11].

The behavior of soil-structure interaction effects in the analysis of structures founded on the surface or embedded in the soil is still one of the most discussed issues in the field of seismic design. The importance of underground structures such as nuclear power plants, underground tunnels is required that the design should be such that it can withstand safely in severe conditions. For a safe design, several artificial boundaries have been studied in the literature and can be mostly classified into

Local (Viscous), Consistent boundaries. Local boundary conditions are commonly used in engineering practice because the radiation condition is satisfied approximately at the artificial boundary, as the solution is local in space and time. On the other hand, consistent boundaries such as Lysmer and Wass [1] and [12] have mathematically complex formulations and satisfy exactly the radiation condition at the artificial boundary. Lysmer and Kuhlemeyer [6] recommended a system of dashpots (independent of wave frequency) known as the viscous boundary, positioned at an artificial boundary, which can absorb both harmonic and non-harmonic scattering waves effectively. Lysmer and Wass [1] proposed a transmitting boundary (dependent on the frequency), which is intended to absorb body waves and surface waves on the lateral infinite boundary. Kosloff and Kosloff [13] proposed the technique which absorbs radiating wave from the interior region to outward on the absorbing region around about an interior region. The first model has been analyzed with three boundaries conditions, viz. viscous, consistent, and infinite boundaries. In developing cities, the underground tunnels for transport facilities (subways, underpasses, sewers, etc.) are being constructed on a large scale. A lot of buildings have been constructed directly above or near the underground tunnels. The complex behavior of the reinforced concrete structures in the presence of underground tunnels and their vulnerability to earthquakes have been the major topic of interest for the past few years among structural engineering researchers. Nonlinear time history analysis is the most rigorous technique to compute seismic responses. However extensive studies have been done by various researchers [14–17], on the effects of tunneling, stability of tunnels, and on interactions between tunnels and overground constructions. Major research studies have aimed to predict the movement of the earth around the tunnels through experimental, analytical, and numerical methods. The seismic response of a soil-structure system during an earthquake is affected by many factors including the soil type and its parameters (shear modulus, mass density, and damping), structure height, and its materials properties in addition to the frequency content of the earthquake and soil-structure interaction [16, 23]. Analytically described the impact of the tunnel excavation on the adjacent structures using PLAXIS-2D software under seismic loading conditions. Mangushev et al. [18] investigated the role of deep excavation and its effects on nearby existing buildings for shallow foundations. Korff [19] described the axial pile deformation due to the vertical soil displacement and observed that deep excavations may cause settlement and damage to adjacent buildings even if the building is situated on deep piles.

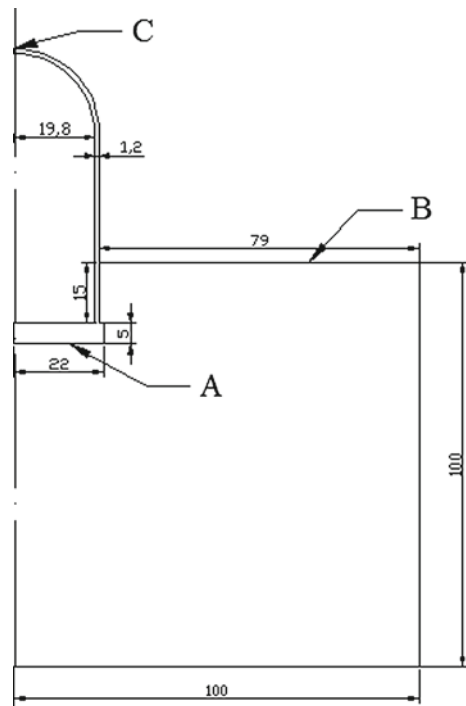
The present study aims at understanding the seismic behavior of multi-storeyed buildings standing in proximity to an underground tunnel excavation and also to determine the influence of an underground tunnel excavation on the response of the nearby building subjected to earthquake excitation. The analytical study has been carried out using finite element by modeling the building-tunnel-soil system.

2 Statements of Problem

In numerical modeling, boundary conditions plays an important role. To study the dynamic SSI on underground structures, two models have been considered using ABAQUS 6.14. The models are validated with the [6] boundary condition. Further results have been compared with two more boundary conditions, viz. Novak and Mitwally [20] boundary and Bettess [21] Infinite element boundary. The three boundary conditions will be called further as BC-1, BC-2, and BC-3 corresponding to Lysmer and Kuhlemeyer [6], Novak and Mitwally [20], and Bettess [21], respectively. The problems which have been considered are as follows:

- I. Outer containment shell of a typical nuclear reactor building with an embedment in surrounding soils Fig. 1.
- II. Seismic performance of multistoried buildings constructed in proximity to an underground tunnel excavation and influence of underground tunnel excavation on the response of the nearby building subjected to earthquake excitation.

Fig. 1 Model with embedment



2.1 Example I: Nuclear Reactor Building

It consists of a reinforced concrete cylindrical shell capped with a spherical dome and resting on a raft. The geometrical properties of the model are the height of the structure from the base of the foundation to the top of the superstructure is 72.9 m, the base of the foundation is 22 m in width, and thickness of the foundation is 5 m, the thickness of the superstructure is 1.2 m, the distance from the axis of symmetry to the inner part of the shell of the structure is 19.8 m. Material properties of containment shell and soil are shown in Table 1 [22]. For non-linearity, Mohr–Coulomb material model is used. For soil modeling, an 8-noded quadrilateral element in plane strain condition is used. For containment shell ‘shell element’ is used.

Nuclear power plant founded on soft soil is modeled using finite elements and dynamic analysis is carried out. To rationally consider SSI, the unbounded soil needs to be modeled properly for this, Lysmer and Kuhlemeyer [6], Novak and Mitwally [20], and Bettess [21] boundary conditions are used and referred to as BC-1, BC-2, and BC-3, respectively. Further dynamic analysis is carried out considering no embedment and embedment effect. A time history of maximum acceleration of 0.13 g is applied at the base of the system. The frequency of the system is observed and also the effect of embedment with (SSI) is compared with no embedment with SSI.

Table 1 Properties of Material Parameters

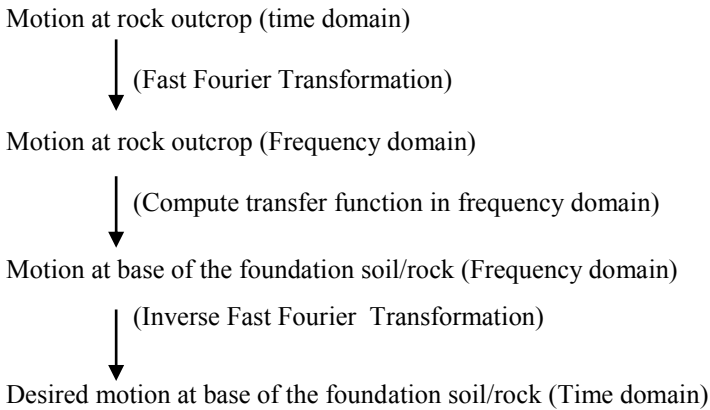
<i>Properties of Soil</i>	
Modulus of elasticity	$25 \times 10^3 \text{ kN/m}^2$
Poisson’s ratio	0.35
Unit weight of Soil	1700 kg/m^3
Damping in soil	15%
Rayleigh damping Co-efficient α and β	0.2805 & 0.1212
Dilation angle	0.1
Shear Modulus	$250 \times 10^6 \text{ N/m}^2$
Cohesion	$7 \times 10^6 \text{ N/m}^2$
Friction angle	37^0
Slope angle	45^0
<i>Properties of containment shell</i>	
Modulus of elasticity	$25 \times 10^6 \text{ kN/m}^2$
Poisson’s ratio	0.25
Unit weight of Soil	2400 kg/m^3
Damping in soil	5%

2.1.1 Numerical Analysis and Modeling

For the analysis, the model was assumed without embedded in its surrounding soil, and its response was compared with that of the same model embedded in the surrounding soil. A site-specific data of the Northridge earthquake (1994) having the maximum acceleration of 0.29 g has been taken as the input motion. But this, acceleration time history can't be directly put on the surface of the ground as an input motion.

This observed input motion is applied at the base of the foundation soil/rock, i.e., 100 m depth so the ground motion must be de-convoluted to get the input response at the base of the soil/rock. The basic stipulation of the de-convolution is shown in Fig. 2.

The procedure of de-convolution can be easily understood through the following steps:



After de-convolution of the motion, the peak value of the acceleration is reduced to 0.13 g (Pro-Shake's User Manual) which is shown in Fig. 3.

There are two cases for the analysis part: one is without embedment and part two is with embedment. The width of soil is considered 100 m from the axis of symmetry

Fig. 2 De-convolution of Motion

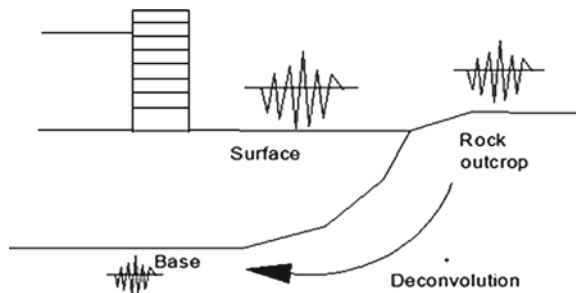
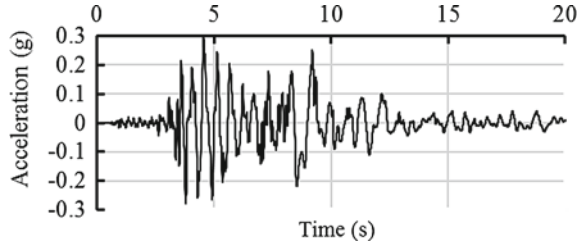


Fig. 3 Northridge (1994) earthquake acceleration-time history



and depth has also been considered 100 m from the base of the foundation. In case of no embedment, only the base foundation will come under the contact of soil. But in case of the embedment, it is assumed that 15 m of structural part from the top of the base of the foundation is embedded in the soil. All this information regarding geometrical data and without embedment and with embedment conditions of the model are shown in Fig. 4a, b, respectively.

For the analysis, the model was assumed without embedded in its surrounding soil, and its response was compared with that of the same model embedded in the surrounding soil. Therefore, two cases were assumed.

- (1) Without embedment of structure in the surrounding soil and
- (2) With embedment of structure in the surrounding soil.

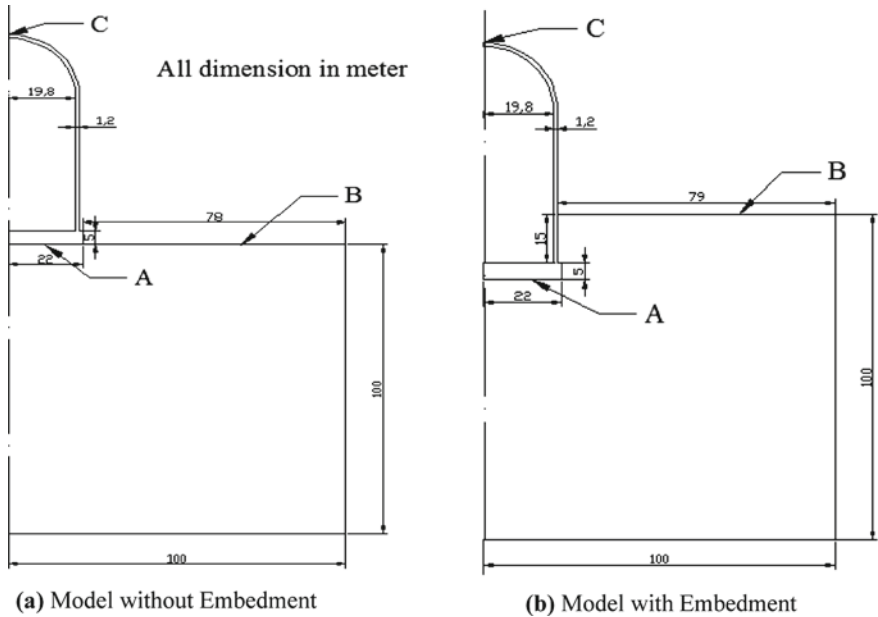


Fig. 4 Model for Analysis

Various points are indicated in Fig. 4 as A, B, and C. All these notations are used for getting the response of the system. In Fig. 4, point A represents a node between the foundation and soil media interface. Point B is representing a node in the soil media and it is named as free-field (FF). Point C represents a node that is the topmost nodal point of the structure. Point A can be treated as an interface, Point B can be treated as FF, and Point C can be treated as the crest. Two cases, i.e., without embedment and with embedment were considered for the response of the structure, with the above discussed boundaries.

The response was obtained with the FEM meshing of the model using ABAQUS. The shell element is used for the analysis of the system, because the shell element gives better results for the axisymmetric system. The response was obtained in terms of acceleration and displacement corresponding to applied time history.

2.1.2 Response of the System

In this section, first the effect of soft soil is considered then the effect of different boundary conditions is examined. The effect of different boundary conditions is carried out without embedment and with embedment. The effect of these boundary conditions is expressed in terms of acceleration and displacement response. The response has also been plotted for top node C of the structure and tabulated for three nodes A, B, C.

2.1.3 Effect of Soft Soil on the Response

The response of the structure is compared for two cases, when situated on soft soil and assumed to be situated on a rock. Table 2 shows the response obtained without embedment effect when the structure is on rock and soil. It can be observed from Table 2 that due to the presence of soft soil, the response at each node increases significantly. The acceleration at node C is observed 0.55 g and displacement as 65 mm for node C when situated on the soil.

Table 2 Responses of Structure situated on Rock and Soil

Without Embedment Structure is Situated on				
Nodes	Rock		Soil	
	Acceleration (g)	Displacement (mm)	Acceleration (g)	Displacement (mm)
A	0.14	15	0.18	20
B	0.16	20	0.26	35
C	0.30	50	0.55	65

Table 3 Response of the system

Response Points	BC-1 [6]		BC-2 [20]		BC-3 [21]	
	Without Embedment	With Embedment	Without Embedment	With Embedment	Without Embedment	With Embedment
<i>Acceleration response</i>						
A	0.29	0.19	0.20	0.18	0.175	0.15
B	0.38	0.28	0.36	0.26	0.22	0.20
C	0.53	0.48	0.51	0.45	0.49	0.42
<i>Displacement response</i>						
A	26	19	19	16	18	12
B	36	31	33.4	29	31	22
C	72	64	69	58	64	50

Table 4 Time period of system (sec)

Modes	Without embedment		With embedment
	Structure on rock	Structure on soil	Structure on soil
1	0.153	0.428	0.408
2	0.108	0.343	0.310
3	0.089	0.192	0.187

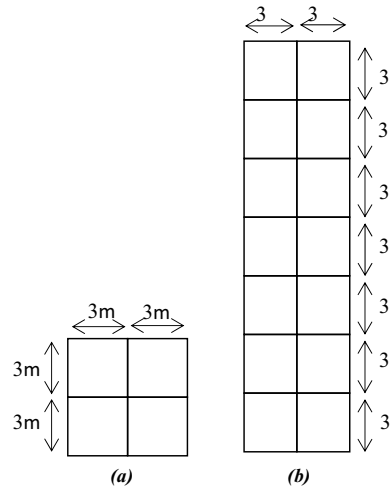
2.1.4 Effect of Embedment

In this section, various boundaries were used at the boundary of the soil media to get the response without embedment and with embedment, respectively. Our main focus is to show the variation of acceleration response of point C of the NPP system. Without embedment and with embedment, acceleration time history is plotted for node C which is as follows (see Table 3).

2.1.5 Time Period of the System

The time period of the system is calculated for the first three modes. Initially, it is assumed that the structure is situated on the rock though its stiffness is high, so its natural frequency will be high. When the structure is situated on the rock without embedment, the time period for the first mode is 0.153 s and decreased for further modes. When the structure is situated on the soft soil, the system gets less stiff than the previous case, so its frequency decreased by some amount hence time period of the system increased more. Further, when the structure is embedded in the soil medium its stiffness would be more than the without embedment. Since frequency is more in the case of embedment hence the time period of the system decreased by some amount. Table 5 shows the time period of all three modes of the system. It can

Fig. 5 a Plan and b elevation of the building



be observed from the Table 5 that as structure gets stiffer its time period decreased. Due to the embedment of the structure in the surrounding soil, the time period is observed for the first mode is 0.408 s (Table 4)

2.2 Example II: Multistoreyed Building in Proximity to an Underground Tunnel Excavation

The building consists of 7-storey two-bay moment-resistant frame building whose two storeys are situated under the ground (like basement). The plan and elevation of the building are shown in Fig. 5. Each storey height is taken as 3 m. The cross sections of columns and beams are taken as $0.3 \text{ m} \times 0.3 \text{ m}$. Three different types of foundation systems, viz. isolated footing, mat footing, and pile foundation are taken for the study. The dimensions of each isolated and mat footings are considered as $2 \text{ m} \times 2 \text{ m} \times 1 \text{ m}$ and $8 \text{ m} \times 8 \text{ m} \times 1 \text{ m}$, respectively. The depth and diameter of the pile foundation considered are 10.0 m and 1.0 m, respectively. The foundation can be visualized as a beam resting on the soil mainly responsible for distributing the structural load uniformly to the soil. The diameter of the tunnel in all cases is taken as 8 m. It is located 11 m below the ground level. Four different horizontal tunnel locations with respect to the center line of the building are considered below the ground surface. These four horizontal distances are 0, 5, 10, 15 m from the centre line of the building.

The mass of this building has been considered to be concentrated at each floor level and the floor systems were assumed to be rigid rectangular floors supported by relatively massless, axially inextensible columns. The building has been analyzed as a 2D frame. Beams and columns have been modeled as two-noded beam elements.

The performance of deep excavations is strongly influenced by the soil behavior. In finite element analysis, it is absolutely important to use realistic soil models [22, 24] to obtain more consistent results. ABAQUS includes several basic models for soils (e.g., Mohr–Coulomb, Drucker-Prager, and Modified Cam clay). In this study, the Mohr–Coulomb plasticity is used to model slipping and gapping of the soil elements because it is a criterion used to model the inelastic behavior of soils.

The bottom of the soil is assumed as bedrock where ground motions were applied for the analysis and assumed fixed. The properties of the bedrock were considered the same as for concrete. The two-dimensional soil was simulated as a rectangle with 160 m width and 32 m depth. The soil under the building has been modeled and meshed as the 8-noded quadrilateral plane strain elements.

For numerical analysis of wave propagation, the size of an element (Δl) should satisfy the condition as per Eq. (1) so that numerical distortion of transmitted waves is avoided [6]

$$\Delta l \leq \frac{\lambda}{10} \sim \frac{\lambda}{8} \quad (1)$$

where λ is the wavelength of the transmitted wave in the soil model and it is related to the shear wave velocity of the soil and the highest frequency of the input motion (f_{\max}) by the following relation:

$$\lambda = \frac{v_s}{f_{\max}} \quad (2)$$

In order to achieve convergence in computations, size of the element (Δl) has been taken as 1.1 m. The finite element meshing for different positions of the tunnel is shown in Fig. 6. Considering Eqs. (1–2), shear wave velocity of the soil is 850 m/s and the highest frequency of the input motions adopted is 25 Hz. The properties of soil and concrete used for the analysis are presented in Table 5.

2.2.1 Soil-Foundation Interface Modeling

In ABAQUS, mechanical contact between the soil and foundation system can be modeled either as node-based interaction or surface-based interaction. In surface-based interaction, mechanical contact of soil and foundation has been modeled using surface elements. Surface-based interaction is suitable because of its capability to model both normal and tangential interaction behavior. Generally, interface modeling has three steps: (a) definition of the contact surfaces which could potentially be in contact, (b) identification of master and slave surfaces that interact with one another, (c) definition of the mechanical (tangent and normal) and thermal properties of the surface. In the surface-based contact approach, two surfaces are required to be defined based on their rigidity; the more deformable surface is defined as a slave surface and the more rigid surface is defined as a master surface. Master surfaces should be

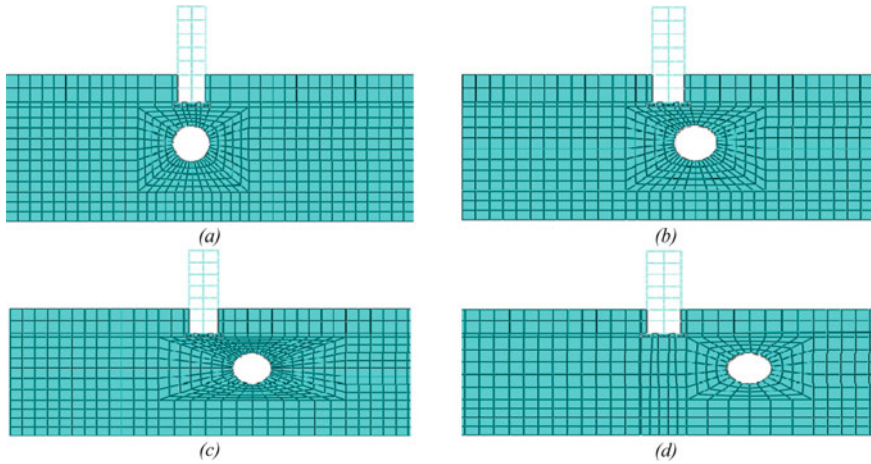


Fig. 6 Meshing of soil and building models with tunnel positions at **a** 0 m **b** 5 m **c** 10 m **d** 15 m

Table 5 Properties of soil and concrete

Parameters	Density (kg/m ³)	Modulus of elasticity (GPa)	Poisson's ratio (ν)	Cohesion (MPa)	Friction angle	Dilation angle	Grade
Soil	2050	4.0	0.30	7.0	0	0	–
Concrete	2400	48.3	0.15	–	–	–	M25

defined as element-based surface. However, slave surfaces can be defined as either element based or node-based surfaces. In this study, the foundation and soil were considered as master and slave surfaces, respectively.

2.2.2 Input Excitations

In this study, the acceleration time histories of the El-Centro, 1979 (PEER 2013) and Moravian Disaster Response (MDR), 2014 earthquakes were used for numerical analyses, as shown in Fig. 7. In order to consider the influence of different seismic wave inputs on the structural system, seismic wave excitations are considered acting horizontally from the bedrock.

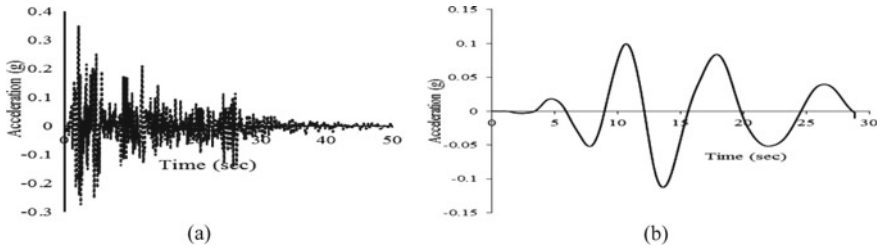


Fig. 7 a El-Centro N-S b MDR earthquake motion

2.2.3 Analysis and Results

The analysis has been carried out for the whole soil structure-foundation system using ABAQUS 6.14 considering the three foundation types. Rayleigh damping coefficients have been considered in which damping parameters of the soil and concrete have been taken through frequency analysis. For calculating Rayleigh damping coefficients, the damping of soil and concrete was taken to be 20% and 5%, respectively. The Rayleigh viscous damping coefficient for a given frequency ω_i can be expressed in terms of critical damping, ξ_i , as

$$\xi_i = \frac{\alpha}{2\omega_i} + \frac{\beta\omega_i}{2} \quad (3)$$

where α and β are the Rayleigh damping coefficients. For calculation of the value of α and β , first two modes of natural frequencies of the building standing on the soil-tunnel system ω_1 and ω_2 were considered. In this study, the value of α and β was calculated using Eq. (3) for each case by considering the frequency analysis of the structure soil-tunnel system. The above procedure has been considered for the buildings with the three types of foundations (mat foundation, isolated foundation, and pile foundation) for the study of the response of the structures. The response computations were carried out for two cases. Both El-Centro and MDR earthquake ground motions as mentioned earlier were used to calculate the displacements of the buildings. The whole analysis of soil, tunnel, and structure interaction was carried out in two steps. In the first step, only gravity load was used whereas in the second step dynamic implicit step for earthquake analysis was used. The peak displacements experienced by the building with and without tunnel excavations were determined to study the impact of the position of the underground tunnel on the seismic displacement of the building. In the first case, the seismic analysis of the building before excavating the underground tunnel was done. In the second case, the dynamic analysis of the building system was carried out, in the presence of the underground tunnel.

The peak displacement experienced on the top-left corner node c of the structure under different tunnel positions is shown in Fig. 8 under MDR earthquake loading

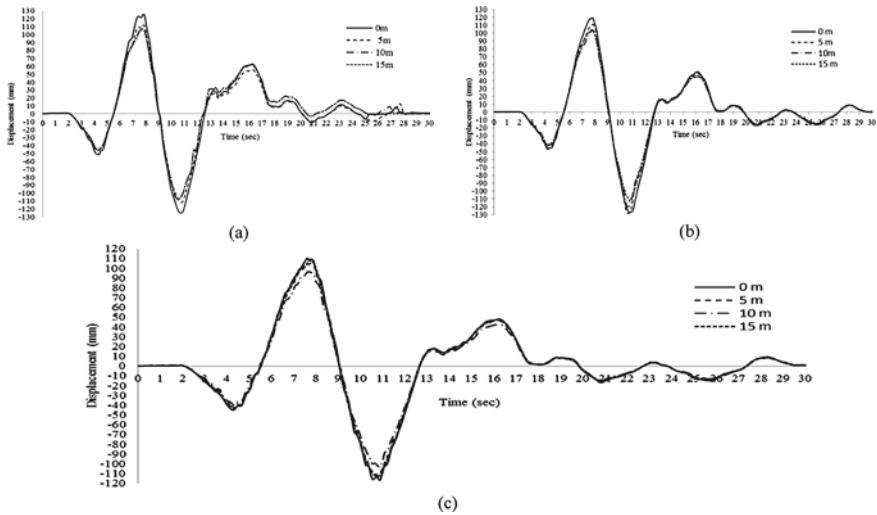


Fig. 8 Displacement Time history for **a** Isolated and **b** Mat and **c** Pile Foundation

for isolated and mat foundation in presence of varying horizontal tunnel locations of 0, 5, 10, 15 m from the center line of the building frame.

The maximum peak displacement for various tunnel positions and also for different types of foundation systems experienced by the building due to MDR earthquake excitation are presented in Table 6. The peak displacement of the building with an isolated foundation is 6.048% more than that of the building with the mat foundation in absence of tunnel condition.

It is seen that the peak displacement of the building system is decreasing when the tunnel is shifted away from the center line of the building. The comparative values of peak displacements under MDR earthquake are shown in Fig. 9.

The comparative study of maximum displacement of building top-left corner for different foundation systems due to El-Centro earthquake is shown in Fig. 10.

Further, Table 7 presents the maximum displacement experienced by the building due to the El-Centro earthquake for different types of foundation systems and the tunnel positions. It is seen that the maximum displacement experienced by the building system is in the case of an isolated foundation when the tunnel is located at the center line of the building.

Finally, the impact of the underground tunnel on the adjacent buildings during different earthquake loadings can be evaluated. Table 8 represents the comparative changes of maximum seismic displacement before tunnel and after tunnel.

Table 6 Maximum peak displacement (mm) at a constant vertical depth of 11 m below ground level

Position of tunnel	Isolated foundation	Increase relative to no tunnel	Decrease relative to 0 m	Mat foundation	Increase relative to no tunnel	Decrease relative to 0 m	Pile foundation	Increase relative to no tunnel	Decrease relative to 0 m
No tunnel	105.45	0.00	-	102.96	0.00	-	99.24	0.00	-
0	119.19	13.74	0.00	118.85	15.89	0.00	109.08	9.84	0.00
5	112.15	6.70	7.04	111.07	8.11	7.78	104.86	5.62	4.22
10	107.40	1.95	11.79	105.25	2.29	13.60	101.65	2.41	7.43
15	106.81	1.36	12.38	104.42	1.46	14.43	100.58	1.34	9.27

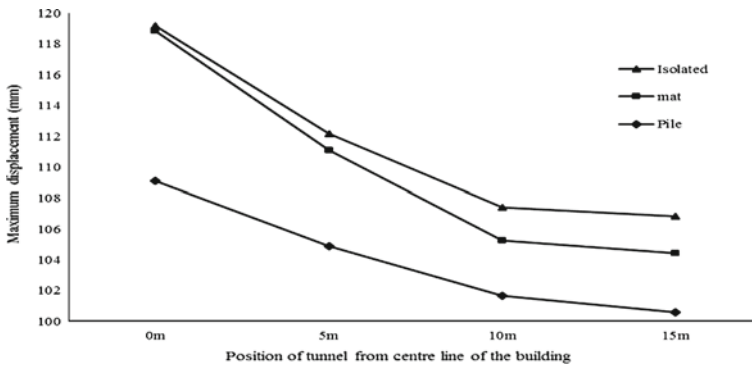


Fig. 9 Maximum displacement versus position of the tunnel under MDR earthquake

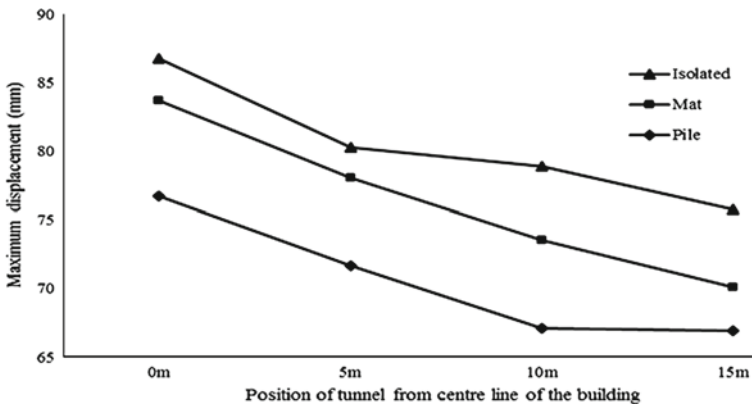


Fig. 10 Maximum displacement of building top for different lateral positions of the tunnel

2.2.4 Discussion of the Result

When the tunnel is shifted away from the center line of the building, it is observed that the peak displacement of the building system is decreasing. From the study, it is observed that maximum displacement was experienced when frame models are situated on an isolated foundation system. From Table 8, it was clearly observed that the maximum displacement occurs in the case of MDR earthquake irrespective of the El-Centro earthquake for all cases of structures.

Table 7 Maximum displacement (mm) at top of building for various horizontal tunnel positions due to El-Centro earthquake

Position of tunnel	Isolated foundation	Increase relative to no tunnel condition	Decrease relative to 0 m	Mat foundation	Increase relative to no tunnel condition	Decrease relative to 0 m	Pile foundation	Increase relative to no tunnel condition	Decrease relative to 0 m
No tunnel (m)	70.17	0.00	-	69.88	0.00	-	66.70	0.00	-
0	86.74	16.57	0.00	83.72	13.84	0.00	76.71	10.01	0.00
5	80.25	10.08	6.49	78.05	8.17	5.67	71.66	4.96	5.05
10	78.90	8.73	7.84	73.56	3.68	10.16	67.09	0.39	9.62
15	75.74	5.57	11.00	70.12	0.24	13.60	66.92	0.22	9.79

Table 8 Comparison of changes in maximum seismic displacement of building before and after tunnel placement due to El-Centro and MDR earthquakes excitation

Earthquakes	No. of storeys	Max. seismic displacements before the tunnel (mm)	Max. seismic displacements after tunnel (mm)	Changes in max. displacement (mm)	Percentages of changes in max displacements (%)
El-Centro	7 storey	70.17	86.74	16.57	23.61
MDR	7 storey	105.45	119.19	13.74	13.03

3 Summary

An analytical study has been presented to demonstrate the displacement response of a reinforced concrete building frame founded on isolated, mat, and pile foundations and standing over the soil through which an underground tunnel runs at a constant depth. The response was also studied when the off-center tunnel positions change. A seven-storey building along with a soil-tunnel system was modeled with viscous boundary conditions and the system was analyzed using ABAQUS software under El-Centro and MDR earthquake excitations. The results show that when the tunnel is located directly below the center line of the building, the maximum influence on the building response is obtained. For this position of the tunnel, the interaction between soil, tunnel, and building structure is the most significant and produces maximum displacement. The displacement response of the building decreases with the increasing horizontal position of the tunnel from the center line of the building. Also, considering the mat, isolated, and pile foundations system, the isolated foundation system produces maximum response irrespective of the spacing of the tunnel positions. The response of the building in each case is maximum when the building is situated on the isolated footing. The study confirms that the building responses in presence of the underground tunnel depend on the tunnel position.

4 Conclusions

1. The response of an NPP structure situated on soil is considerably higher than that situated on the rock. For the case considered here, the response increased by a margin of about 67%.
2. The time period of the system decreases due to the embedment effect of structure which indicates that the system is stiffer.
3. The acceleration and displacement responses of the system, are smaller with the infinite boundary as compared to kelvin and viscous boundary.
4. The maximum influence on the building is observed when the tunnel is located directly below the center line of the building.

5. The displacement response of the building decreases with the increasing horizontal position of the tunnel from the center line of the building.
6. The isolated foundation system produces maximum response irrespective of the spacing of the tunnel positions.

Future Recommendations Future studies can be extended considering different soil conditions, structure types, and structure heights.

References

1. Lysmer J, Waas G (1972) Shear waves in plane infinite structures. ASCE. [https://doi.org/10.1016/S0895-7177\(98\)00155-1](https://doi.org/10.1016/S0895-7177(98)00155-1)
2. Beskos DE (1987) Boundary element methods in dynamic analysis. *Appl Mech Rev ASME* 40:1–23
3. Wolf JP, Song C (1995) Doubly asymptotic multi-directional transmitting boundary for dynamic unbounded medium-structure-interaction analysis. *Earthq Eng Struct Dyn*. <https://doi.org/10.1002/eqe.4290240204>
4. Song C, Wolf JP (2002) Semi-analytical representation of stress singularities as occurring in cracks in anisotropic multi-materials with the scaled boundary finite-element method. *Comput Struct* 80(2):183–197
5. Basu U, Chopra AK (2003) Perfectly matched layer for time-harmonic elastodynamics of unbounded domains: theory and finite-element implementation. *Comput Methods Appl Mech Eng*. [https://doi.org/10.1016/S0045-7825\(02\)00642-4](https://doi.org/10.1016/S0045-7825(02)00642-4)
6. Lysmer J, Kuhlemeyer L (1969) Finite-dynamic model for infinite media. *J Eng Mech Div*
7. Clayton W, Engquist B (1980) Geophysics. Absorbing Bound Condition Wave Equ Migr. <https://doi.org/10.1190/1.1441094>
8. Zienkiewicz OC, Emson C, Bettess P (1983) A novel boundary infinite element. *Int J Numer Meth Eng* 19(3):393–404
9. Bettess P (1977) Infinite elements. *Int J Numer Methods Eng*
10. Lio ZP, Wong HL (1984) A transmitting boundary for the numerical simulation of elastic wave propagation. *Int J Soil Dyn Earthq Eng*. [https://doi.org/10.1016/0261-7277\(84\)90033-0](https://doi.org/10.1016/0261-7277(84)90033-0)
11. Al Assady AKMS (2005) Modeling of nonlinear dynamic soil-structure interaction problems. PhD dissertation, Indian Institute of technology Roorkee, Roorkee, India
12. Kausel E (1994) Thin-layer method: formulation in time domain. *Int J Numer Meth Eng* 37:927–941
13. Kosloff R, Kosloff D (1986) Absorbing boundaries for wave propagation problems. *J Comput Phys* 10.1016/0021-9991(86)90199-3
14. Besharat V, Davoodi M, Jafari MK (2012) Effect of underground structures on free-field ground motion during earthquakes. In: *Proceedings of 15th world conferences on earthquake Engineering*, pp 1–10
15. Abdullah MH, Taha MR (2013) A review of the effects of tunneling on adjacent piles. *Electron J Geotech Eng* 18N:2739–2762
16. Azadi M, Hosseini M (2014) The influence of tunnels on the nearby buildings under seismic loadings conditions, case study: Shiraz underground-Iran. *Proc 14th World Conf Earthq Eng* 1–8
17. Bhatkar T, Barman D, Mandal A, Usmani A (2016) Prediction of behaviour of a deep excavation in soft soil: a case study. *Int J Geotech Eng* 6362:1–10. <https://doi.org/10.1080/19386362.2016.1177309>

18. Mangushev R, Rybnov E, Lashkova E, Osokin A (2016) Examples of the construction of deep excavation ditches in weak soils. *Procedia Eng* 165:673–681. <https://doi.org/10.1016/j.proeng.2016.11.765>
19. Korff M (2009) Deformations and damage to buildings adjacent to deep excavations in soft soils 143
20. Novak M, Mitwally H (1988) Transmitting boundary for axisymmetric dilation problems. *J Eng Mech Div ASCE* 104(4):953–956
21. Bettess P (1977) Infinite elements. *Int J Numer Meth Eng* 11:53–64
22. Farghlay AA (2014) Evaluation of seismic performance of buildings constructed on hillside slope of Dronka village—Egypt. *Int J Geotech Eng* 9(2)
23. Cong S, Tang L, Ling X et al (2018) Boundary effect on the seismic response of a three-dimensional soil slope with a shallow foundation on top. *KSCE J Civ Eng* 22:1130–1140. <https://doi.org/10.1007/s12205-017-1535-4>
24. Kumar A, Choudhury D (2016) DSSI analysis of pile foundations for an oil tank in Iraq. *ICE Proceed Geotech Eng* 169(2):129–138. <https://doi.org/10.1680/jgeen.15.00025>